The effect of mode coupling on ballistic electron transport in quantum wires

1991 J. Phys.: Condens. Matter 3 5729

(http://iopscience.iop.org/0953-8984/3/30/006)

J. Phys.: Condens. Matter 3 (1991) 5729–5740. Printed in the UK

The effect of mode coupling on ballistic electron transport in quantum wires

K Nakazato† and R J Blaikie‡

† Hitachi Cambridge Laboratory, Cavendish Laboratory, Madingley Road, Cambridge CB3 0HE, UK

‡ Microelectronics Research Centre, Cavendish Laboratory, Madingley Road, Cambridge CB3 0HE, UK

Received 12 October 1990, in final form 1 May 1991

Abstract. Ballistic electron transport in arbitrarily shaped wires is modelled by the conversion processes of elementary quantum modes. The resistance quantization and geometrical resonances are calculated in cavity structure embedded in a quantum wire. At the resonant points, which correspond to virtual bound states, mode coupling becomes essential and the propagation of one mode is enhanced and blocked by the virtual bound state of the other, resulting in the appearance of a pair of resonant and anti-resonant peaks. The phase shift of the scattering matrix is shown to be a powerful indicator for analysing the coupling among quantum modes.

1. Introduction

Current nanofabrication technology enables us to fabricate semiconductor devices in which quantum effects in transport and the wave nature of the electrons become apparent. One such important technology is to confine the electrons of a two-dimensional electron gas (2DEG) in a semiconductor heterostructure to regions with a lateral extent of 100 nm or less, resulting in narrow quantum wires, constrictions, and quantum dots. The Fermi wavelength of the confined electrons is close to the dimension of these nanostructures, so the quantization due to the standing waves becomes very important. Also, the small size of the structures and the very high mobility of the parent 2DEG make the electron transport ballistic at low temperatures. Striking examples of the novel physical phenomena in these ballistic nanostructures are the recent experimental observations of resistance quantization in point-contact structure (Wharam *et al* 1988, van Wees *et al* 1988), periodic conductance resonances in a cavity (van Wees *et al* 1989, Meirav *et al* 1990), and one-dimensional bandstructure in quantum dot lattices (Kouwenhoven *et al* 1990a, Kouwenhoven *et al* 1990b, Haug *et al* 1990). Although many resonant and anti-resonant peaks have been observed in these structures, the nature of these resonances has not been clearly understood.

Ballistic transport in quantum wires has been studied by many authors (Szafer and Stone 1989, Kirczenow 1989, Yosefin and Kaveh 1990, Ulloa *et al* 1990, Brum 1990). A quantum wire is divided into a sequence of boxes and the wavefunctions are connected by matching the boundary conditions at the interfaces between the boxes. Using this method electron transport has been studied for simple geometries. However, it is rather

0953-8984/91/305729 + 12 $03.50

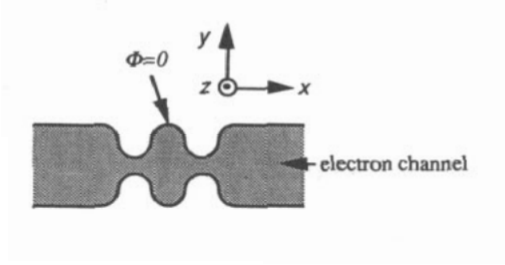

Figure 1. Plan view of a semiconductor wire. The wavefunction of electrons Φ vanishes at the quantum wire boundary.

difficult to extend this method to more complicated geometries and to the incorporation of the electric field effect because the matrix dimension becomes quite large.

In this paper the wavefunction is expanded into the elementary quantum modes and the coefficients of these modes are obtained by the transfer matrix method. The element of the transfer matrix describes the conversion process among the elementary quantum modes. This coupled-mode transfer matrix method makes it possible to calculate the electron transport in arbitrarily shaped quantum wires and to include the electric field effect, although this paper only treats the former situation. Particular attention is focused on the resistance in cavity structure, because this is the fundamental element for constructing more complicated structures such as quantum dot lattices.

2. Scattering formalism

The system under consideration is very simple. Electrons are confined at the surface in the z direction (e.g. 2DEG) and propagate in the x, y directions. The wavefunctions of the electrons vanish at the boundary of the quantum wire as shown in figure 1. Such quantum wires have been fabricated by several methods—Schottky gate depletion (Thornton *et al* 1986), FIB induced damage isolation (Hiramoto *et al* 1987), etching (Ishibashi *et al* 1988), and biased FIB implanted p-regions (Blaikie *et al* 1991).

The two-dimensional Schrödinger equation is written as

$$-(\hbar^2/2m)(\partial^2/\partial x^2 + \partial^2/\partial y^2)\Phi + V\Phi = E\Phi \tag{1}$$

where $\hbar$ is the Planck constant divided by 2π, m is the electron mass, V is a potential, and E is an energy. The reduction from the three-dimensional Schödinger equation to the two-dimensional Schrödinger equation may be obtained by the decoupled approximations developed in the framework of the envelope function approximation (Brum 1990).

The present configuration is an open system in which electrons are entered or absorbed through electrodes. In such a system the problem is similar to the scattering problem in which the boundary condition is that the wavefunction takes a linear combination of propagating waves into and out of the system. Without loss of generality, in the regions $x < x_L$ and $x > x_R$ it is assumed that quantum wire is a straight line parallel to the x axis and the potential V is constant. The electron channel of quantum wire is defined by $y_1(x) > y > y_2(x)$ as shown in figure 2.

The wave function takes the following form for $x < x_L$:

$$\Phi = \sum_{j=1}^{n} \frac{1}{\sqrt{k_j(x_L)}} (a_{jL} \exp(ik_j(x_L)(x - x_L)) + b_{jL} \exp(-ik_j(x_L)(x - x_L))c_j(x_L|y) \tag{2a}$$

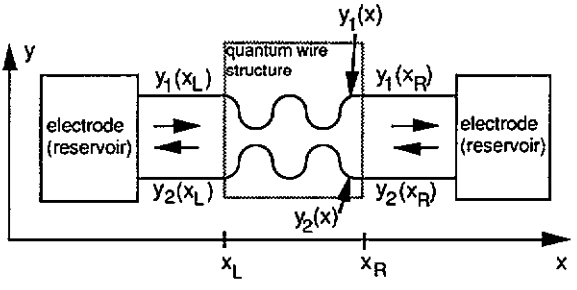

Figure 2. Configuration of the system. A quantum wire structure is connected to two electrodes which are modelled by ideal reservoirs.

and for $x > x_R$,

$$\Phi = \sum_{j=1}^{n} \frac{1}{\sqrt{k_j(x_R)}} (a_{jR} \exp(ik_j(x_R)(x-x_R)) + b_{jR} \exp(-ik_j(x_R)(x-x_R)))c_j(x_R|y) \quad (2b)$$

where c_j is a complete set of orthonormalized functions in y direction along the line of constant x,

$$c_j(x|y) = \sqrt{\frac{2}{y_1(x)-y_2(x)}} \cos\left[\frac{\pi j}{y_1(x)-y_2(x)}\left(y - \frac{y_1(x)+y_2(x)}{2}\right)\right] \qquad j = 1,3,5,\ldots \quad (3a)$$

$$c_j(x|y) = \sqrt{\frac{2}{y_1(x)-y_2(x)}} \sin\left[\frac{\pi j}{y_1(x)-y_2(x)}\left(y - \frac{y_1(x)+y_2(x)}{2}\right)\right] \qquad j = 2,4,6,\ldots \quad (3b)$$

and k_j is the longitudinal wave number in the direction of the quantum wire given by

$$k_j(x) = \sqrt{(2m/\hbar^2)(E - \bar{V}(x)) - [\pi j/(y_1(x)-y_2(x))]^2} \quad (4)$$

$$\bar{V}(x) = \frac{1}{y_1 - y_2} \int_{y_2}^{y_1} V(x,y)\,dy. \quad (5)$$

In equation (2), n is the maximum integer for which k_n has a real value. For the notational simplicity, the same n is assumed in $x < x_L$ and in $x > x_R$, although the extension to the case of different n is straightforward.

Coefficients a_j and b_j defined by equation (2) are related by the scattering matrix S,

$$\begin{pmatrix} b_{iL} \\ a_{iR} \end{pmatrix} = \sum_{j=1}^{n} \mathbf{S}(i,j) \begin{pmatrix} a_{jL} \\ b_{jR} \end{pmatrix}. \quad (6)$$

The vector on the right-hand side of the above equation represents the incoming wave and the vector on the left-hand side represents the outgoing wave. The scattering matrix **S** is a $2n$ by $2n$ matrix written by the transmission and reflection coefficients as follows,

$$\mathbf{S}(i,j) = \begin{pmatrix} r_L(i,j), t_R(i,j) \\ t_L(i,j), r_R(i,j) \end{pmatrix}. \quad (7)$$

The density matrix of the system is defined by

$$\rho(r,r') = \sum_i \Psi_i(r) f_i \Psi_i^*(r') \quad (8)$$

where Ψ_i is a complete set of eigenfunctions and f_i is the distribution function. It is

assumed that there are no real bound states in the quantum wire. This means that the wavefunctions, the asymptotic form of which is given by equation (2), can construct a complete set of the system. By taking the following eigenfunctions,

$$\Phi_{i\rightarrow}: \text{boundary condition } (\forall j | a_{jL} = \sqrt{k_i(x_L)}\delta_{ij}, b_{jR} = 0) \tag{9a}$$

$$\Phi_{i\leftarrow}: \text{boundary condition } (\forall j | a_{jL} = 0, b_{jR} = \sqrt{k_i(x_R)}\delta_{ij}) \tag{9b}$$

the density matrix (8) is given by

$$\rho(r, r') = \frac{m}{\pi\hbar^2}\sum_{i=1}^{n}\left(\int_{V_{iL}}^{\infty}\Phi_{i\rightarrow}(r)f_L\Phi_{i\rightarrow}^*(r')\frac{dE}{k_i(x_L)} + \int_{V_{iR}}^{\infty}\Phi_{i\leftarrow}(r)f_R\Phi_{i\leftarrow}^*(r')\frac{dE}{k_i(x_R)}\right) \tag{10}$$

where

$$\begin{aligned} V_{iL} &= \bar{V}(x_L) + (\hbar^2/2m)(\pi i/(y_1(x_L) - y_2(x_L)))^2 \\ V_{iR} &= \bar{V}(x_R) + (\hbar^2/2m)(\pi i/(y_1(x_R) - y_2(x_R)))^2. \end{aligned} \tag{11}$$

Here f_L and f_R are the distribution functions of the left and right incoming waves. The quantum wire is connected to two electrodes which are modelled well by black bodies. That is, electrons emerge from an electrode with its local equilibrium distribution, and electrons entering an electrode are absorbed completely. The electrodes are assumed to be ideal reservoirs characterized by their chemical potentials, E_{FL} and E_{FR}, which are given by the external biases, V_L and V_R, as

$$E_{FL} = E_F - qV_L \qquad E_{FR} = E_F - qV_R \tag{12}$$

where E_F is the equilibrium Fermi energy and q is the absolute value of electron charge. The density matrix gives electric current density,

$$J(r) = -q(\hbar/2mi)(\partial/\partial r - \partial/\partial r')\rho(r, r')|_{r=r'}. \tag{13}$$

The density matrix (10) and the electric current density (13) give the total electric current in the quantum wire. Since the total current is conserved along the quantum wire, it can be estimated just outside of the electrodes using the asymptotic form equation (2). From the black body distribution with chemical potentials (12), the total current in the quantum wire is given by

$$I = \int_{y_2}^{y_1} j_x\,dy = -\frac{q}{\pi\hbar}\int_{-\infty}^{\infty}\mathcal{T}(E)(f(E + qV_L) - f(E + qV_R))\,dE \tag{14}$$

where $f(E)$ is the Fermi–Dirac distribution function and $\mathcal{T}(E)$ is the transmission probability defined by

$$\begin{aligned} \mathcal{T}(E) &= \sum_{i,j=1}|t_R(i,j)|^2\theta(E - V_{iL})\theta(E - V_{jR}) \\ &= \sum_{i,j=1}|t_L(j,i)^2\theta(E - V_{iL})\theta(E - V_{jR}). \end{aligned} \tag{15}$$

Here θ is the step function ($\theta(x) = 0$ when $x < 0$ and $\theta(x) = 1$ when $x > 0$) and the time-reversal symmetry of the scattering matrix is used.

The scattering theory gives a complete set of orthonormalized eigenfunctions in the quantum wire which satisfy the boundary conditions, and the reservoir nature of electrodes gives the distribution of these eigenfunctions. These are the essentials of the

Landauer formulation. However, the latter assumption may be replaced by the rate equations when the scattering among eigenfunctions or many-body effects become important. Even in this case the eigenfunctions obtained by the scattering theory may still play an important role as a basis in the electron transport.

3. Approximations

In the quantum wire structure, the wavefunction is expanded by the complete set (3),

$$\Phi(x, y) = \sum_{i=1}^{\infty} \chi_i(x) c_i(x|y). \tag{16}$$

The coefficient χ_i obeys a matrix equation and the coupling of different modes occurs according to the boundary variation of the quantum wire. The details are described in appendix 1. The matrix equation is solved and the scattering matrix obtained gives the total current using equations (14) and (15). Although the dimension of the matrix of the equation is infinite, the scattering matrix converges quickly after the maximum mode number exceeds $n + 2$ where n is a maximum integer for which the wave number k_n finds a real value in the quantum wire.

In this paper the electric field effect is neglected in the calculations so that the potential, V, is equal to zero throughout the system. Furthermore the potential difference between two electrodes is assumed to be small so that equation (14) gives a resistance R,

$$\frac{1}{R} = \frac{1}{R_q} \int_{-\infty}^{\infty} \mathcal{T}(E) \left(-\frac{\partial f(E)}{\partial E} \right) \mathrm{d}E. \tag{17}$$

Here the resistance quantum R_q is equal to $h/2q^2$. At absolute zero temperature the resistance is simply given by the transmission probability at equilibrium Fermi energy, $R = R_q/\mathcal{T}(E_F)$. The effect of finite temperature is to average the transmission probability around the Fermi energy within a width of $k_B T$.

When the scattering and electron–electron interactions are neglected, the Schrödinger equation (1) and the resistance expression (17) are invariant by the following scaling transformation,

$$x \to \lambda x \qquad E \to \lambda^{-2} E \qquad T \to \lambda^{-2} T. \tag{18}$$

This scaling relation suggests that in smaller structures ($\lambda < 1$) quantum effects may be observed at higher temperatures. Furthermore, this scaling allows us to fix the length of quantum wires in our calculations since similar shaped quantum wires give the same results by scaling the energy according to equation (18). In this paper the width of the quantum wire will be fixed at 100 nm and the transmission probability $\mathcal{T}(E)$ which gives the conductance at absolute zero temperature will be discussed.

4. Calculation of conductance in cavity structure

Figure 3 shows the results for a cavity structure, which is a quantum dot structure embedded in a quantum wire, the plan view of which is shown in the inset. The width of the quantum wire is 100 nm and the width of two constrictions is defined by W. When $W = 0$ the quantum dot becomes a square. In calculation the effective mass of the electron is assumed to be that of GaAs, $0.067\, m_0$ where m_0 is the electron mass in

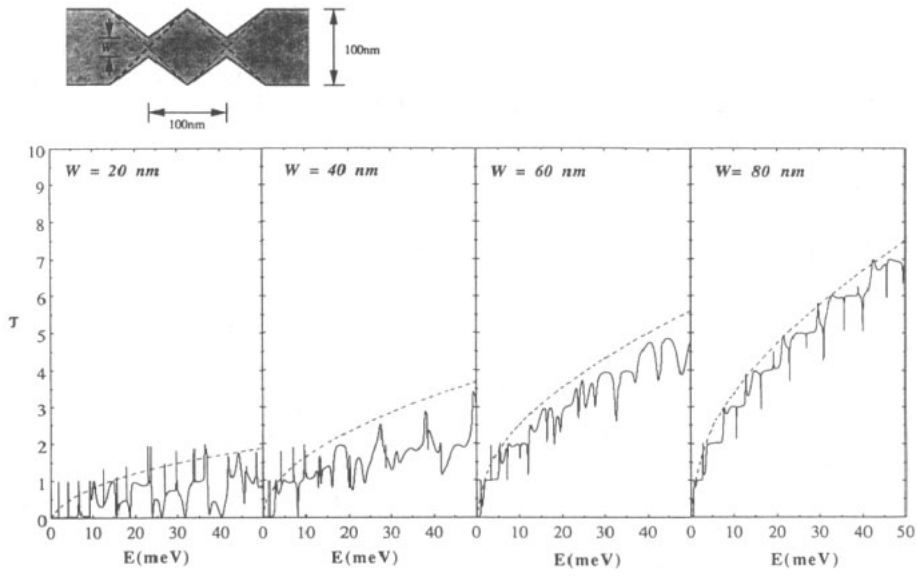

Figure 3. Transmission probability in cavity structures. The dotted line indicates the classical conductance.

vacuum. The overall character of the conductance is described by a classical expression for the conductance with the width W, $R_q/R = k_F W/\pi$, where $k_F = \sqrt{2mE}/\hbar$ is the Fermi wavelength. Around the classical value, the conductance *fluctuates* with amplitude $1/R_q$, similar to universal conductance fluctuations under a magnetic field (Lee and Stone 1985).

This conductance fluctuation consists of many sharp resonances and anti-resonances. A rough estimation of these resonant points is obtained by a non-coupling approximation. When the coupling among different modes is neglected, the wavefunction of the jth mode follows the one-dimensional Schrödinger equation in a potential,

$$V_j = \bar{V}(x) + (\hbar^2/2m)[\pi j/(y_1(x) - y_2(x))]^2. \tag{19}$$

The WKB approximation gives a quantum condition,

$$\int_{\text{Cavity}} k_j(x)\,\mathrm{d}x = (n + \gamma)\pi \qquad n = 0, 1, \ldots \tag{20}$$

where the integral is taken in the region that $k_j(x)$ has a real value in the cavity. A constant γ takes a value between $\frac{1}{2}$ and 1, depending on the shape of the potential V_j. In the case of figure 3, the shape changes linearly near constrictions and the constant γ is nearly equal to $\frac{1}{2}$.

Figure 4 shows the effect of mode-coupling. The resonant peaks are characterized by a pair of quantum numbers (j, n) in equation (20). Important effects of mode-coupling are the shift of the resonance energy and the appearance of anti-resonances. Besides the shift and the anti-resonances the non-coupling picture explains the main features of the transmission probability. The origin of anti-resonance is as follows. When the energy becomes high, a lower mode starts to propagate by incoherent tunnelling through two

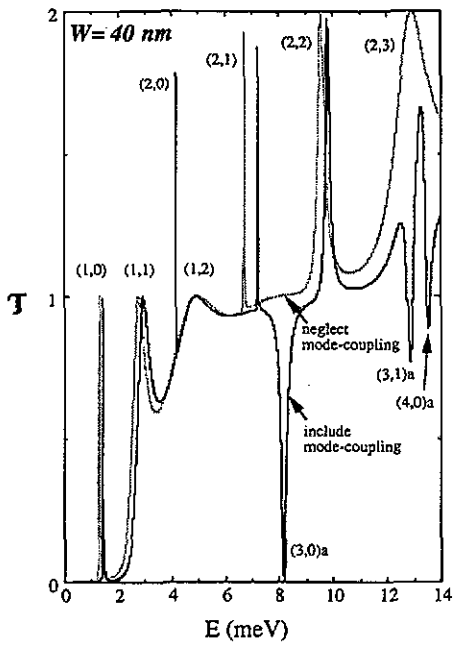

Figure 4. Effect of mode coupling on the transmission probability of a cavity structure. The resonant peaks are characterized by two quantum numbers (j, n) in equation (20). 'a' means anti-resonance.

constrictions as shown in figure 5. The transmission probability has a finite value, but there is no coherence between the two tunnelling events at the constrictions. When there is a virtual bound state of a higher mode in the cavity, coupling between the propagating lower mode and the virtual bound state occurs. The wavefunctions of the propagating lower mode and the virtual bound state of higher mode are denoted by φ_l and φ_h. There are two possible combinations of the wavefunctions, $\varphi_l \pm \varphi_h$. One of these two combinations assists the coherent tunnelling of lower propagating mode, resulting in a resonant peak if the transmission is less than 1 (figure 5(a), (b)). However, if the channel of the lower mode is completely opened, that is, the transmission is 1, there is no effect on the transmission probability (figure 5(c)). The other combination prevents the propagation of the lower mode, resulting in an anti-resonance. This anti-resonance appears when the channel of the lower mode is opened (figure 5(b), (c)).

In order to clarify the situation it is very useful to discuss the eigenvalues of the scattering matrix. By the unitarity condition the eigenvalue has unit modulus and may be written $\exp(2i\delta)$ with real δ. Figure 6 shows the phase shift, δ, as a function of energy. The phase shift gives the phase change through the quantum wire and has a similar meaning to the wave number. The phase-shift diagram (figure 6) therefore gives a dispersion relation of the quantum modes in quantum wire. The resonant point is characterized by the point that the phase shift δ takes a value close to 0 and $\pi/2$. Around the resonant points the phase shift changes value by π. If there is another propagating mode, crossing of the corresponding phase shifts occurs, resulting in a strong coupling of two modes as is clearly shown at points (2,2) (3,0) in figure 6.

Figure 7 shows the general feature of the energy–longitudinal wave number dispersion relation. In the case of straight quantum wire the dispersion relation consists of several parabolas corresponding to several propagating modes. The energy at $k = 0$ is

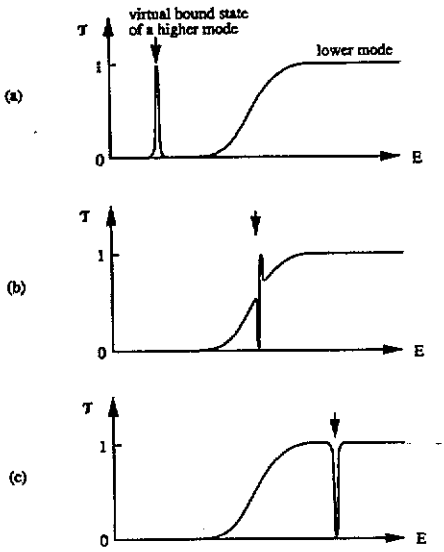

Figure 5. Schematic feature of transmission probability as a function of energy when a lower propagating mode couples with a virtual bound state of a higher mode.

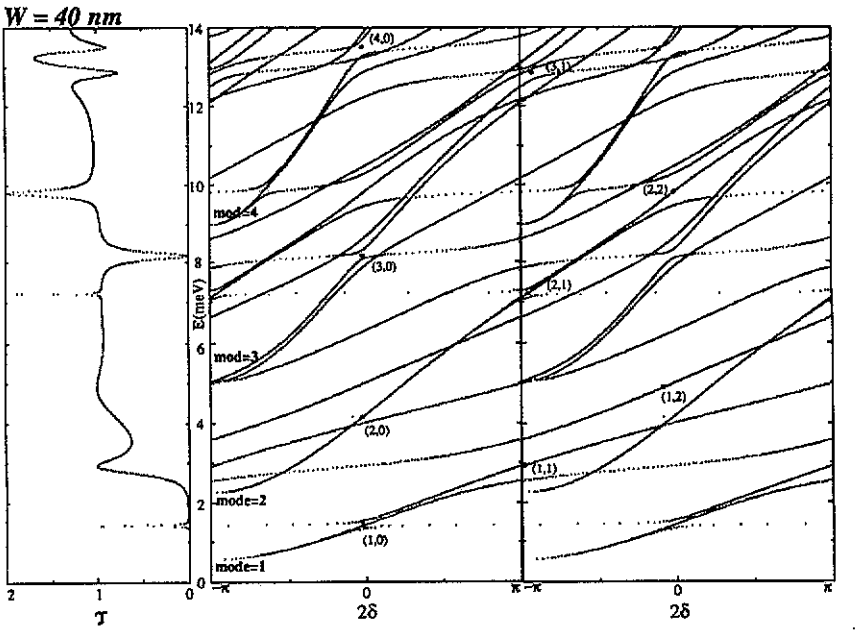

Figure 6. Phase shift diagram of a cavity structure. In order to show the phase shift near $2\delta = \pi$ the same figure is repeated twice. The resonance occurs when phase shift 2δ takes value nearly 0 and π.

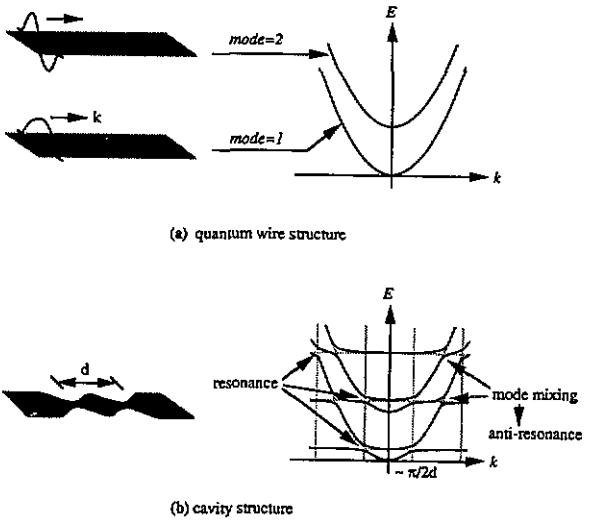

Figure 7. Schematic feature of energy–longitudinal wave number relation of (a) a quantum wire structure and (b) a cavity structure embedded in a quantum wire.

given in equation (19). Introducing a cavity structure in a quantum wire, reflection of electron waves at two constrictions occurs and strong interference results in resonant peaks. The dispersion line becomes flat, similar to band gap formation in solids. At the resonant point, the dispersion line may touch the line of the other mode, and strong mode mixing occurs, resulting in an anti-resonance peak. It should be noted that even infinitesimally small boundary perturbation causes a pair of resonant and anti-resonant peaks. Smaller pertubations give sharper peaks as shown in figure 3.

5. Discussion and conclusion

In this paper the geometrical effect on ballistic electron transport is modelled by the scattering theory and the assumption of ideal reservoirs for electrodes, which are the essentials of the Landauer formulation. The scattering matrix is calculated by the coupled-mode transfer matrix method. An element of the transfer matrix represents the conversion process between elementary quantum modes, which is caused by the variation of the boundary of quantum wire. The resistance quantization and geometrical resonances are calculated by this method. At resonant points in cavity structures strong mode coupling occurs, resulting in the enhancement or blocking of the one-dimensional propagation by 0-dimensional virtual bound state of different mode. The phase shift is shown to be a powerful method for analysing the coupling among these quantum modes. Furthermore, resonances can be characterized by special value of phase shift as shown in figure 6, which may lead to a general argument of electron transport in quantum wires.

There are many problems to be solved in future work. For example, the electric potential effect, multi-connection structures such as rings, electron–electron interactions, and so on. An important problem to be solved in future works is a Coulomb interaction effect among electrons in the quantum wire, since the electrons are fully

confined and the small structures may reduce the confined electrons so that the transport may be influenced strongly by the existence of other background electrons.

Recently, bandstructures in quantum dot lattices have been observed (Kouwenhoven *et al* 1990a,b, Haug *et al* 1990). In the quantum wire structures it is possible to integrate arbitrary 'material' having designed energy gap and effective mass. In this case the inverse scattering theory may become an important tool in the design of such artificial 'material'.

Acknowledgments

The authors thank Dr H Ahmed, Dr J R A Cleaver and Mr G J Goodings of the University of Cambridge, and Mr H Mizuta and Dr D A Williams of Hitachi Cambridge Laboratory for many helpful discussions.

Appendix 1. Coupled-mode transfer matrix method

Insertion of equation (16) to the Schrödinger equation (1) gives

$$\frac{d^2}{dx^2}\chi_i + \sum_{j=1}^{\infty}\left(2C_{ij}^{(1)}\frac{d}{dx}\chi_j + C_{ij}^{(2)}\chi_j + K_{ij}\chi_j\right) = 0 \tag{A1}$$

where

$$C_{ij}^{(n)} = \int_{y_2}^{y_1} c_i(x|y)\frac{\partial^n}{\partial x^n}c_j(x|y)\,dy \tag{A2}$$

$$K_{ij} = k_i^2\delta_{ij} - \frac{2m}{\hbar^2}\int_{y_2}^{y_1} c_i(x|y)(V(x,y) - \bar{V}(c))c_j(x|y)\,dy. \tag{A3}$$

By a transformation

$$\chi_i = \sum_{j=1}^{\infty} M_{ij}f_j \tag{A4}$$

where

$$\mathbf{M} = \exp\left(-\int^x C^{(1)}(x')\,dx'\right), \tag{A5}$$

equation (A1) becomes

$$\frac{d^2}{dx^2}f_i = -\sum_{j=1}^{\infty}\omega_{ij}f_j \tag{A6}$$

with

$$\omega_{ij} = \sum_{m,n=1}^{\infty}(M^{-1})_{im}K_{mn}M_{nj}. \tag{A7}$$

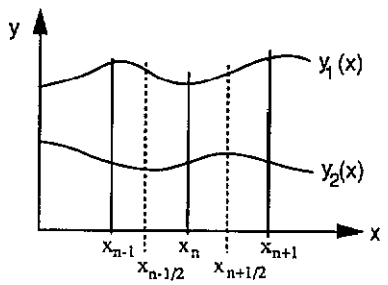

Figure A1. Coordinate of calculation.

The above equation can be solved by dividing the plan pattern of the quantum wire into segments as shown in figure A1. We approximate the constant ω in each segment,

$$\omega_{ij}(x) = \omega_{ij}(x_{n+1/2}) \qquad \text{for } x_n \leqslant x < x_{n+1}. \tag{A8}$$

When the electric potential effect is neglected, the matrix **K** defined by equation (A3) is diagonal and the wave function in the segment n is given by

$$\Phi^{(n)}(x,y) = \sum_{i,j=1}^{\infty} M_{ij}(x, x_{n+1/2}) \frac{1}{\sqrt{|k_j^{(n)}|}} [a_j^{(n)} \exp(ik_j^{(n)}(x - x_{n+1/2})) + b_j^{(n)} \exp(-ik_j^{(n)}(x - x_{n+1/2}))] c_i(x|y) \tag{A9}$$

where $\mathbf{M}(x_1, x_2)$ is

$$\mathbf{M}(x_1, x_2) = \mathbf{M}(x_1)\mathbf{M}(x_2)^{-1} = \exp\left(-\int_{x_2}^{x_1} C^{(1)}\,dx\right) \simeq \left(1 - \frac{1}{2}\int_{x_2}^{x_1} C^{(1)}\,dx\right)\left(1 + \frac{1}{2}\int_{x_2}^{x_1} C^{(1)}\,dx\right)^{-1}. \tag{A10}$$

Equation (A10), based on the Cayley transform, satisfies the condition $\mathbf{M}^{\mathrm{T}}\mathbf{M} = \mathbf{1}$ which guarantees total current conservation, and is valid up to the second order of $\Delta y_1/(y_1 - y_2)$ and $\Delta y_2/(y_1 - y_2)$ which is consistent with the approximation (A8). The explicit form of the coefficient $C^{(1)}$ is

$$C_{ij}^{(1)} = \begin{cases} 0 & i = j \\ (-1)^{(i-j)/2} \dfrac{2ij}{i^2 - j^2} \dfrac{1}{y_1 - y_2} \dfrac{\mathrm{d}}{\mathrm{d}x}(y_1 - y_2) & i + j = \text{even}, i \neq j \\ (-1)^{(i+j+1)/2} \dfrac{2ij}{i^2 - j^2} \dfrac{1}{y_1 - y_2} \dfrac{\mathrm{d}}{\mathrm{d}x}(y_1 + y_2) & i + j = \text{odd}. \end{cases} \tag{A11}$$

By the connection rule that the wavefunction and its x derivative are continuous at x_n, the coefficients a, b are obtained successively,

$$\begin{pmatrix} a_i^{(n)} \\ b_i^{(n)} \end{pmatrix} = \sum_{j=1}^{\infty} \mathbf{T}^{(n)}(i,j) \begin{pmatrix} a_j^{(n-1)} \\ b_j^{(n-1)} \end{pmatrix} \tag{A12}$$

where

$$\mathbf{T}^{(n)}(i,j)=\begin{pmatrix} \dfrac{k_i^{(n)}+k_j^{(n-1)}}{2k_i^{(n)}}\exp[-ik_i^{(n)}(x_n-x_{n+1/2})+ik_j^{(n-1)}(x_n-x_{n-1/2})], & \dfrac{k_i^{(n)}-k_j^{(n-1)}}{2k_i^{(n)}}\exp[-ik_i^{(n)}(x_n-x_{n+1/2})-ik_j^{(n-1)}(x_n-x_{n-1/2})] \\ \dfrac{k_i^{(n)}-k_j^{(n-1)}}{2k_i^{(n)}}\exp[ik_i^{(n)}(x_n-x_{n+1/2})+ik_j^{(n-1)}(x_n-x_{n-1/2})], & \dfrac{k_i^{(n)}+k_j^{(n-1)}}{2k_i^{(n)}}\exp[ik_i^{(n)}(x_n-x_{n+1/2})-ik_j^{(n-1)}(x_n-x_{n-1/2})] \end{pmatrix}$$
$$\times\sqrt{\left|\frac{k_i^{(n)}}{k_j^{(n-1)}}\right|}\,M_{ij}(x_{n+1/2},x_{n-1/2}). \tag{A13}$$

The total transfer matrix is given by

$$\mathbf{T}=\mathbf{T}^{(N)}\mathbf{T}^{(N-1)}\ldots\mathbf{T}^{(1)}. \tag{A14}$$

Here $x_1=x_{1/2}=x_L$ and $x_N=x_{N+1/2}=x_R$. The transfer matrix obtained has elements in which k_j takes an imaginary value. The boundary condition is that there are no growing modes outside the quantum wire, $a_R^{(I)}=b_L^{(I)}=0$, where (I) means the elements corresponding to the imaginary value of k_j, and the sign of the imaginary wave number is defined by $ik_j>0$. Using this boundary condition, a $2n$ by $2n$ transfer matrix and the scattering matrix are obtained.

References

Blaikie R J, Nakazato K, Fraboni B, Hasko D G, Cleaver J R A and Ahmed H 1991 *Microelectron. Eng.* **13** 373

Brum J A 1990 *20th Int. Conf. on the Physics of Semiconductors* p 2363

Huag R J, Lee K Y, Smith III T P and Hong J M 1990 *20th Int. Conf. on the Physics of Semiconductors* ed E M Anastassakis and J D Joannopoulos (Singapore: World Scientific) p 2443

Hiramoto T, Hirakawa K, Iye Y and Ikoma T 1987 *Appl. Phys. Lett.* **51** 1620

Ishibashi K, Takagi Y, Gamo K, Namba S, Takaoka S, Murase K, Ishida S and Aoyagi Y 1988 *J. Vac. Sci. Technol.* B **6** 1852

Kirczenow G 1989 *J. Phys.: Condens. Matter* **1** 305

Kouwenhoven L P, Hekking F W J, van Wees B J and Harmans K J P M 1990a *Phys. Rev. Lett.* **65** 361

Kouwenhoven L P, van Wees B J, van der Enden B and Harmans K J P M 1990b *20th Int. Conf. on the Physics of Semiconductors* ed E M Anastassakis and J D Joannopoulos (Singapore: World Scientific) p 2325

Lee P A and Stone A D 1985 *Phys. Rev. Lett.* **55** 1622

Meirav U, Kastner M A and Wind S J 1990 *Phys. Rev. Lett.* **65** 771

Szafer A and Stone A D 1989 *Phys. Rev. Lett.* **62** 300

Thornton T J, Pepper M, Ahmed H, Andrews D and Davies G J 1986 *Phys. Rev. Lett.* **56** 1198

Ulloa S E, Castano E and Kirczenow G 1990 *Phys. Rev.* B **41** 12350

Yosefin M and Kaveh M 1990 *Phys. Rev. Lett.* **63** 2819

van Wees B J, van Houten H, Beenakker C W J, Williamson J G, Kouwenhoven L P, van der Marel D and Foxon C T 1988 *Phys. Rev. Lett.* **60** 848

van Wees B J, Kouwenhoven L P, Harmans C J P M, Williamson J G, Timmering C E, Broekaart M E I, Foxon C T and Harris J J 1989 *Phys. Rev. Lett.* **62** 2523

Wharam D A, Thornton T J, Newbury R, Pepper M, Ahmed H, Frost J E F, Hasko D G, Peacock D C, Ritchie D A and Jones G A C 1988 *J. Phys. C: Solid State Phys.* **21** L209